Tropical Oceanic Response to Extratropical Thermal Forcing in a Coupled Climate Model: A Comparison between the Atlantic and Pacific Oceans*

HAIJUN YANG AND LU WANG

Laboratory for Climate and Ocean-Atmosphere Studies, and Department of Atmospheric and Oceanic Sciences, School of Physics, Peking University, Beijing, China

(Manuscript received 7 July 2010, in final form 22 January 2011)

ABSTRACT

The tropical oceanic response to the extratropical thermal forcing is quantitatively estimated in a coupled climate model. This work focuses on comparison of the responses between the tropical Atlantic and Pacific. Under the same extratropical forcing, the tropical sea surface temperature responses are comparable. However, the responses in the tropical subsurface in the two oceans are distinct. The tropical subsurface response in the Atlantic can be twice of that in the Pacific. The maximum subsurface temperature change in the tropical Pacific occurs in the eastern lower thermocline, while that in the tropical Atlantic occurs in the west and well below the lower thermocline. The different responses in the tropical Atlantic and Pacific are closely related to the different changes in the meridional overturning circulations. The Pacific shallow overturning circulation, or the subtropical cell, tends to slow down (speed up) in response to the extratropical warming (cooling) forcing. The changes in the upwelling in the eastern equatorial Pacific as well as the shallow subduction from the extratropical southern Pacific along the eastern boundary are accountable for the eastern Pacific temperature change. The Atlantic overturning circulation consists of the shallow subtropical cell and the deep thermohaline circulation. A weakened thermohaline circulation will result in a strengthened northern subtropical cell, in which the change in the lower branch, or the low-latitude North Brazil Current, can cause strong response below the western tropical thermocline. Here the coastal Kelvin wave along the western boundary on the intermediate isopycnal level also plays an important role in the equatorward conveying of the climate anomalies in the mid-to-high-latitude Atlantic, particularly during the initial stage of the extratropical forcing.

1. Introduction

Tropical–extratropical climate interaction has been one of the main issues of climate research. The tropical climate change has a significant impact on the global climate through the atmospheric bridge, such as quasi-stationary planetary wave or storm tracks (e.g., Lau 1997; Schneider et al. 1997; Alexander et al. 2002). Observational and modeling studies have demonstrated a clear link between sea surface temperature (SST) anomalies in the equatorial Pacific and those in the North Pacific (Zhang et al. 1996; Lau 1997; Zhang et al. 1998; Wang 2002), North tropical Atlantic (Enfield and Mayer 1997), North Atlantic (Hoerling et al. 2001; Lu et al. 2004), and Indian Oceans (Yu and Rienecker 1999) on interannual to decadal time scales. The extratropical climate can also affect the tropics through both the atmospheric bridge and oceanic tunnel (Gu and Philander 1997; Kleeman et al. 1999; Barnett et al. 1999; Pierce et al. 2000), generating decadal to longer-term climate changes, where the oceanic processes are deeply involved in the extratropical-driven tropical low-frequency variability (Matei et al. 2008; Yu and Sun 2009). The extratropical changes can be transported equatorward by mean subduction. The changes in the strength of meridional overturning circulation (MOC) can also alter the tropical temperature by varying the amount of equatorward cold-water transport (Kleeman et al. 1999; Nonaka et al. 2002). The extratropics plays the same important role as the tropics does in the global climate change, particularly on interdecadal and longer time scales.

Quantitative assessment of the tropical–extratropical climate interaction have been made using a fully coupled climate model in our previous studies with focus on

* Department of Atmospheric and Oceanic Sciences Contribution Number 010.

Corresponding author address: Haijun Yang, Department of Atmospheric and Oceanic Sciences, School of Physics, Peking University, 209 Chengfu Rd., Beijing 100871, China.
E-mail: hjyang@pku.edu.cn

DOI: 10.1175/2011JCLI3927.1

the Pacific (Liu and Yang 2003; Yang and Liu 2005). The oceanic dynamics accounts for one-third of the total change in equatorial SST and more than 80% change in equatorial thermocline (Yang and Liu 2005). This tropical response is mainly resulted from ocean circulation adjustment, particularly the subtropical cell (STC) change. The Pacific STC is primarily forced by the midlatitude surface wind (McCreary and Lu 1994), and thus it is strongly coupled with the atmospheric Hadley cell. Because of a lack of deep-water formation, the tropical–extratropical interaction in the Pacific is accomplished by the shallow wind-driven circulation that tends to be symmetric to the equator. Thus, the changes in the tropical ocean also tend to be shallow and symmetric to the equator under the symmetric extratropical forcing.

Quantitative assessment of the extratropical impact on the tropical Atlantic has yet to be clarified. There are lots of observational and modeling studies on how the climate changes in the northern North Atlantic affect the tropical Atlantic (Curry et al. 1998; Zhang and Delworth 2006; Sutton and Hodson 2007; Chang et al. 2008; Zhang et al. 2011). The thermal or freshwater variations in the high latitudes could induce changes in the deep-water formation, causing variations in the Atlantic meridional overturning circulation (AMOC), which affect the tropical Atlantic and beyond (Chang et al. 2008). A recent observational study confirms that the Labrador seawater thickness change can significantly affect the tropical western boundary currents between the lower thermocline and intermediate level through coastal Kelvin waves (Zhang et al. 2011). In the Atlantic, the meridional overturning circulation should include both the wind-driven STC and buoyancy-driven AMOC, and the interaction between them would result in a much more complicate consequence in the tropical–extratropical interaction than that in the Pacific. Previous studies have concluded that the AMOC tends to suppress the northern STC so that only the southern STC is visible in the meridional streamfunction (Zhang et al. 2003; Hazeleger and Drijfhout 2006). The changes in the tropical Atlantic are indeed related to the STC changes, instead of the AMOC (Chang et al. 2008), although the former can be significantly changed by the latter. This reminds us to pay more attention to the wind-driven STC in the study of the tropical Atlantic climate changes.

This work focuses on comparing the tropical responses in the Pacific and Atlantic. Using a so-called partial coupling technique in a fully coupled climate model, sensitivity experiments are performed to quantify the mean climate changes in the tropics. For the tropical SST, the response magnitudes in the tropical Atlantic and Pacific are comparable. However, the responses in the tropical subsurface in the two oceans are very different in both the magnitudes and patterns. The temperature change in the tropical Pacific mainly occurs in the eastern lower thermocline, while that in the tropical Atlantic occurs in the west and well below the equatorial thermocline. The different responses in the tropical Atlantic and Pacific are closely related to the different changes in the MOCs. The AMOC tends to suppress the northern branch of the STC, so that a relaxation in AMOC would result in an enhanced northern STC. This contributes to the strong response in the tropical subsurface Atlantic.

This work can be understood as relevant to the problem of climate adjustment to slow external forcing. The prescribed SST warming in the extratropics is beyond the range of intrinsic coupled variability. However, the strong anomalous signal is necessary in order to generate significant change in the remote region. All the results obtained here are appropriate for our model but could be model dependent. We expect that the physical processes examined here and our understanding of climate adjustment to external forcing can help to understand the reality. This paper is organized as follows: section 2 introduces the coupled model and sensitivity experiments, section 3 examines the general responses in the tropical Pacific and Atlantic, section 4 investigates mechanisms of tropical responses, and the conclusions and a discussion are provided in section 5.

2. Model and experiments

The Fast Ocean–Atmosphere Model (FOAM) is used in this paper. FOAM is developed jointly at University of Wisconsin—Madison and the Argonne National Laboratory (Jacob 1997). The atmosphere model uses the physics of the National Center for Atmospheric Research (NCAR) Community Climate Model, version 3 (CCM3), with a resolution of R15 and 18 vertical levels. The ocean model was developed following the Geophysical Fluid Dynamics Laboratory (GFDL) Modular Ocean Model (MOM) with a resolution of 1.4° latitude × 2.8° longitude × 32 vertical levels. The sea ice component uses the thermodynamics of NCAR's Climate Systems Model (CSM) Sea Ice Model (CSIM) version 2.2.6. This model allows for an ice fraction with growth and melting in leads, snow cover, penetrating radiation with brine pockets and uses a two-layer model for sea ice temperature. Sea ice dynamics is not included. The horizontal resolution of the sea ice model is the same as the ocean model. Without flux adjustment, the fully coupled control simulation (CTRL) has been integrated for over 1000 years, showing no apparent climate drifts. FOAM has been used extensively to simulate the global climate in the past, present, and future. Comprehensive analyses of the model simulation can be found, for example, in Wu et al. (2003) and Yang and Liu (2005).

To quantify the dynamic impact of the climate change in one region on the climate in another remote region, a partial coupling (PC) technique is used in FOAM. Using this approach, full ocean–atmosphere coupling is allowed only in some selected region; elsewhere, the annual cycle of climatological SST from the CTRL is prescribed to force the model atmosphere or ocean. The PC provides an important modeling technique for assessing the individual role of the atmospheric bridge and oceanic tunnel in the interaction between different geographic regions.

Using the similar modeling configuration as in Yang and Liu (2005), we perform three pairs of PC experiments to explicitly quantify the sensitivity of tropical climate to extratropical forcing. All experiments start from the 800th year of the CTRL and are integrated for 200 yr, when the upper ocean has reached quasi-equilibrium. Specifically, the paired PC experiments [i.e., Atmosphere Bridge–Ocean Tunnel (ABOT)] are performed in which a homogenous $\pm 2°C$ ($\pm 4°$, $\pm 8°C$) SST warming is ''seen'' by both the atmosphere and ocean in the extratropics (latitude $> |30°|$) and is then ''carried'' equatorward through both the atmospheric and oceanic bridges. The ocean and atmosphere in ABOT is fully coupled within the tropics (latitude $< |30°|$), but partially coupled in the extratropics where the atmosphere is forced by mean seasonal cycle of heat flux from the CTRL plus a heat flux anomaly originated from the $\pm 2°C$ ($\pm 4°$, $\pm 8°C$) SST anomaly. Here we use P2, P4, and P8 to represent the experiments forced by $+2°$, $+4°$, $+8°C$ SST anomalies, respectively; and M2, M4, and M8 to represent the $-2°$, $-4°$, $-8°C$ cooling experiments, respectively. The residual of the summation [(P + M)/2] is thought to be associated with nonlinearity, while the difference between the warming and cooling experiments [(P − M)/2] is viewed as the linear response. These experiments have the same CTRL run that is performed similarly as the experiments except without the anomalous SST forcing. With the PC technique, the tropical coupled variability cannot feed back to the extratropics, and in turn to be affected by the contaminated extratropical forcing. Thus, the tropical response can be thought as ''purely passive'' response. In general, our results show that a significant impact of the extratropical forcing on the tropical climate. The nonlinear response contributes less than 10% to the forced response in the tropics when compared to the linear response. It is also insensitive to changes in the strength of external forcing (Yang and Wang 2008).

3. General response in the tropical Pacific and Atlantic

The tropical climate can be significantly modulated by the extratropical climate change (Liu and Yang 2003). A warm (cold) SST in the extratropics can force an upper-ocean temperature change of about half the forcing magnitude in the tropics (Fig. 1). As shown in our previous studies (e.g., Yang and Liu 2005), the strong equatorial response occurs because the extratropical impact on tropical climate is accomplished by both the atmospheric bridge of the Hadley cells and the oceanic tunnel of the meridional overturning circulations.

This study focuses on comparing the responses in the tropical Pacific and Atlantic. The general responses show both the similarities and differences (Fig. 1). For the SST, the response in the Atlantic is the same magnitude with that in the Pacific (Fig. 1a). However, for the upper-ocean thermocline, the response in the Atlantic is much stronger than that in the Pacific (Fig. 1b). This stronger Atlantic thermocline response is the problem most interesting to us. We think that both the shallow STCs and the deep AMOC are responsible.

The tropical responses can be also seen in another view (Fig. 2). It is shown that the responses in the tropical SST are proportional to the extratropical forcings for both the Pacific and Atlantic (Fig. 2a). The SST responses change linearly with the extratropical forcings, regardless of the forcing polarity. In Fig. 2 the dashed gray lines represent the magnitude of extratropical forcing and the dark lines for the tropical responses. For the warming and cooling forcing, the tropical SST responses are nearly antisymmetric. This also suggests that the nonlinear response in the tropical SST can be well ignored (Yang and Wang 2008).

The stronger thermocline response in the tropical Atlantic is evident in the Fig. 2b. It is nearly the same magnitude as the extratropical forcing. It is also noticed that the Atlantic response to cooling forcing is smaller than that to warming forcing, showing an apparent asymmetric feature. This suggests that the nonlinear response in the Atlantic thermocline is nontrivial anymore. The asymmetric changed in the AMOC should be responsible (we will return to this later). In contrast, the thermocline response in the tropical Pacific is still linear and symmetric to the extratropical forcing, with the magnitude half of the forcing.

The horizontal patterns show an enhanced equatorial response (EER) in the SST in both the oceans, which dynamics have been discussed in Liu et al. (2005) (Fig. 3a). The patterns also show an enhanced zonal SST gradient in the tropical Pacific and an increased east–west SST contrast in the tropical Atlantic. The enhanced zonal SST contrast in the Pacific is consistent with the ''ocean dynamic thermostat'' paradigm (Clement et al. 1996), in which the cold tongue is controlled by a dynamical feedback where the cold-water upwelling retards the mean temperature increase (Cane et al. 1997). In contrast,

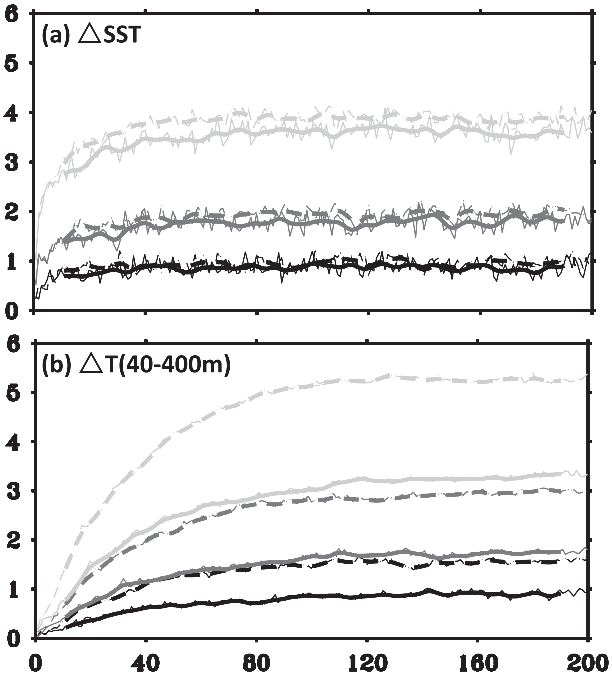

FIG. 1. Evolution of the annual mean linear responses in tropical (a) SST and (b) upper-ocean temperature (40–400 m averaged). The linear responses are calculated as (P − M)/2, in which P (M) represents the anomalies from warming (cooling) experiment. The temperature anomalies are obtained by subtracting the CTRL and averaged within 10°S–10°N. The black, gray, and light gray lines are for 2°, 4°, and 8°C experiments, respectively, in which the solid (dashed) lines are for the Pacific (Atlantic). The 21-yr running mean are also plotted as thick lines.

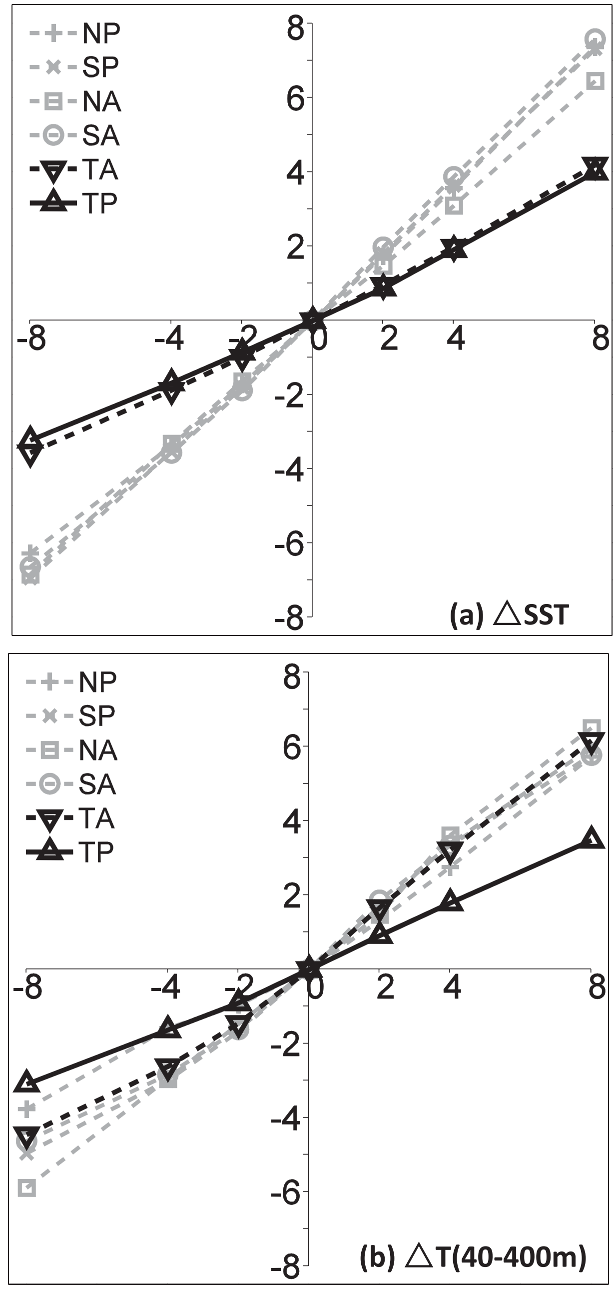

FIG. 2. The responses of the ocean temperature in the Pacific and Atlantic to extratropical forcing for (a) SST and (b) upper-ocean temperature (40–400 m averaged; units in °C). The abscissa represents the magnitude of extratropical forcing while the vertical coordinate represents the oceanic responses. The temperature is averaged over years 151–200 and the mean temperature from CTRL is subtracted. The gray lines show the local changes in the extratropical oceans (N: 40°–60°N, S: 40°–60°S). The black lines show the responses in the tropical oceans (T: 10°S–10°N). The solid (dashed) black lines are for the tropical Pacific (Atlantic).

the SST change in the tropical Atlantic shows a higher warming in the east because of the weak upwelling there.

The subsurface temperature change in the tropical Pacific and Atlantic differs significantly (Fig. 3b). The most remarkable difference is that the tropical Atlantic thermocline also shows an enhanced equatorial response, while the Pacific thermocline shows a reduced response equatorward. Moreover, in the zonal direction, there is bigger (smaller) change in the east (west) in the Pacific and the opposite occurs in the Atlantic for both the warming and cooling experiments. In the Pacific, the oceanic overturning circulation (or the STC) is reduced in response to the weakened Hadley cells in the warming experiments. This requires a westward anomalous temperature gradient to geostrophically balance the poleward anomalous flow at depth (McPhaden and Zhang 2002). In the Atlantic, the changes in the shallow STC and the deep MOC, as well as their interaction, magnify the tropical thermocline response. We will return to this point later with more details.

The vertical structures of the tropical temperature change are also very different in the Pacific and Atlantic

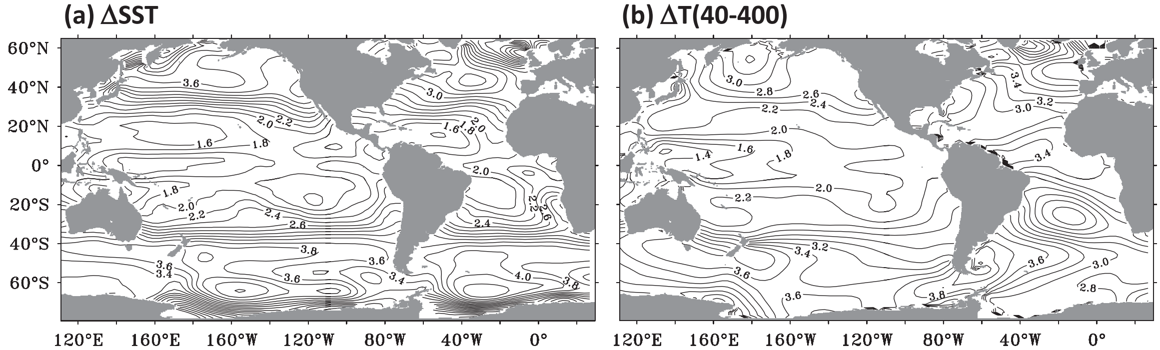

FIG. 3. Horizontal patterns of the temperature changes in (a) the SST and (b) the upper-ocean temperature (40–400 m averaged) for the P4 experiment. The temperature is averaged over years 151–200 and the mean from the CTRL is subtracted. The contour interval (CI) is 0.2°C.

(Fig. 4). The upper-ocean warming in the tropical Pacific is relatively uniform, which mainly occurs above the $26.5\sigma_\theta$ level (0–400 m, Fig. 4a). In comparison, the tropical Atlantic upper-ocean warming shows a strong vertical gradient, where the maximum warming is located at around the $27\sigma_\theta$ level (400–600 m, Fig. 4b). The Atlantic warming is about twice of that in the Pacific, and almost the same magnitude as the extratropical forcing. The uniform upper-ocean warming in the Pacific is related to the significant change in the vertical advection, consistent with the change in the equatorial cells (Liu and Yang 2003). The strong vertical gradient in the Atlantic is consistent with the weak upwelling, where only the meridional advection matters (we will discuss it later). The meridional section also shows a local subsurface maximum warming in the high-latitude Atlantic, which exhibits a baroclinic structure in the vertical near 60°–70°N. This is qualitatively similar to what would happen in high-latitude water hosing experiments. Under the freshwater forcing, a local subsurface warming maximum can be generated as a result of baroclinic response (Mignot et al. 2007). This baroclinic structure is dynamically important because it is closely related to the mechanism and rate of the AMOC recovery once the external forcing is removed (Mignot et al. 2007).

The maximum tropical temperature change occurs in the eastern Pacific and western Atlantic (Fig. 5). This is another significant difference between the two oceans. The maximum warming in the Pacific occurs in the eastern thermocline at the depth of 200 m, which is clearly separated from the surface warming by the strong thermocline as indicated by the dense isopycnal lines. Note that there is a minimum warming in the western thermocline, which is related to the cold-water subduction from the extratropical eastern Pacific (Yang et al. 2005), as well as the flattening of the equatorial thermocline (Yang and Zhang 2008). The maximum warming in the western equatorial Atlantic occurs at the depth of 400–600 m, which is also well separated from the SST change. The temperature change suggests a remote control of the equatorial thermocline. The tropical

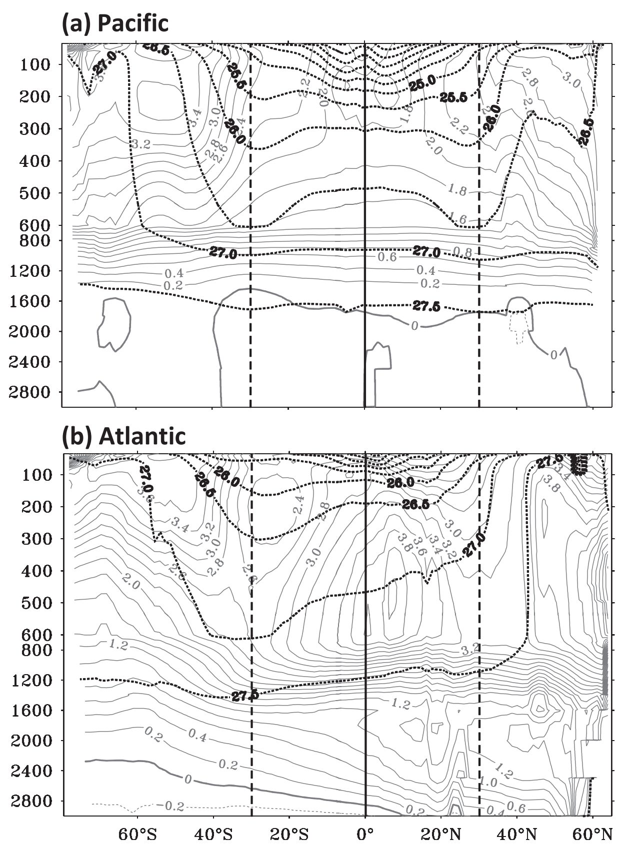

FIG. 4. Zonally averaged temperature changes (solid contours, CI = 0.2°C) in (a) the Pacific and (b) the Atlantic for the P4 experiment. The temperature is averaged over years 151–200 and the mean from the CTRL is subtracted. The dotted contours represent potential density of CTRL (CI = $0.5\sigma_\theta$).

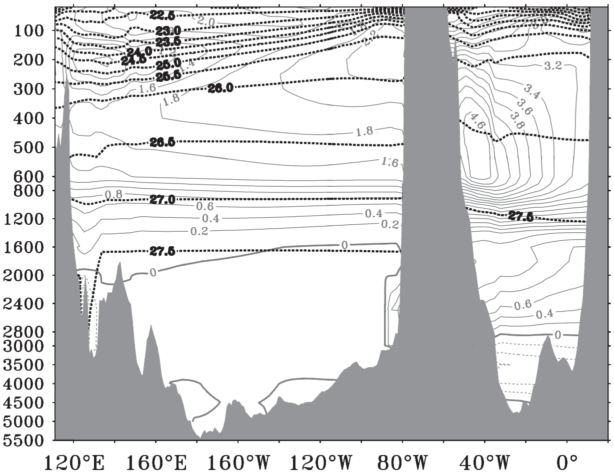

FIG. 5. Tropical mean temperature change (10°S–10°N averaged) for the P4 experiment. (solid contours, CI = 0.2°C). The temperature is averaged over years 151–200 and the mean from CTRL is subtracted. The dotted contours represent potential density of CTRL (CI = $0.5\sigma_\theta$).

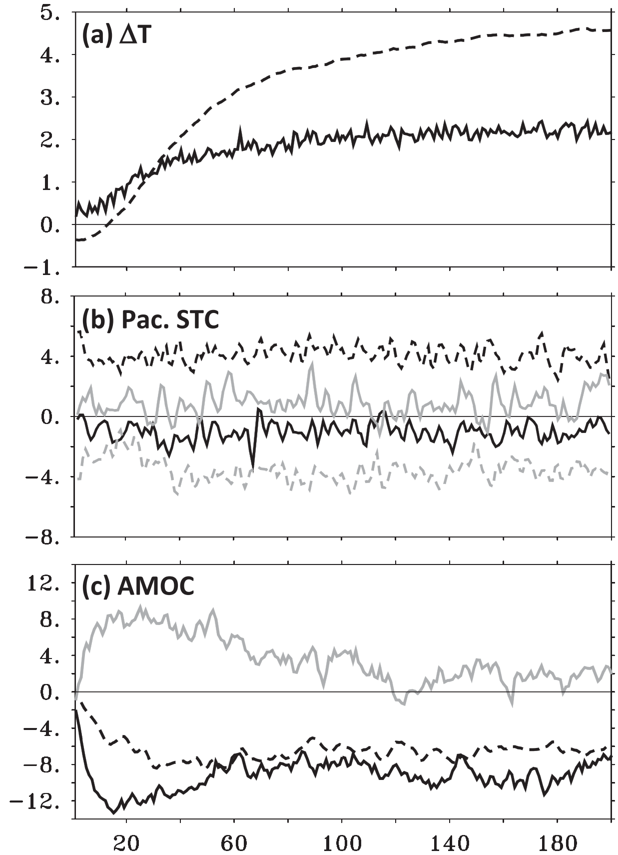

FIG. 6. Time evolution of (a) the temperature changes averaged over subsurface boxes in the Pacific (solid black line) and Atlantic (dashed black line), (b) the Pacific STC, and (c) the AMOC and the volume transport change in the lower branch of the northern Atlantic STC (dashed line) for the P4 experiment. In (a) the Pacific box is defined as 5°S–5°N, 110°–80°W, and 100–300 m and the Atlantic box is defined as 0°–10°N, 60°–30°W, and 400–600 m. In (b) the northern (southern) Pacific STC is defined as the maximum (minimum) of the Pacific meridional streamfunction in the upper 400 m at 0°–20°N (0°–20°S). Solid (dashed) lines are for northern (southern) STC and black (gray) lines are for P4 (M4) experiment (unit: Sv). In (c), the AMOC index is calculated by averaging the streamfunction between 40° and 60°N and 500 and 2000 m. The black (gray) line represents AMOC change in P4 (M4) experiment. The volume transport change in the lower branch of the northern Atlantic STC (dashed line) is calculated by integrating the meridional velocity across the basin along 10°N from 300 to 600 m, as indicated by the dashed black vertical line in Fig. 12b (unit: Sv). The value of the Atlantic STC shown in (c) has been multiplied by a factor of 3. For all lines, the mean values from CTRL are subtracted.

thermocline in the Pacific is related to the shallow-water subduction processes from the subtropics, while that in the Atlantic is related to the intermediate-water subduction or advection, as well as the western boundary coastal Kelvin waves originated in the mid- to high latitudes. We will discuss this in the next section.

The time evolution of the tropical temperature changes shows the different warming rate in the tropical Pacific and Atlantic (Fig. 6a). Although the warming rate in the tropical Pacific (solid line) is smaller than that in the tropical Atlantic (dotted line) during the first several decades, the tropical Pacific reaches the equilibrium much faster than the tropical Atlantic. The equilibrium time scale for the former is about 40 yr, while for the latter the temperature changes significantly even after 80 yr of the onset of the extratropical forcing. The temperature evolutions discussed here are for the subsurface boxes defined in Fig. 6a. Here we should bear in mind that the response speed and time scale is closely related to the circulations, physical processes involved, and the locations. The Atlantic subsurface box is deeper than the Pacific box. This implies a longer equilibrium time scale in the Atlantic due to slower advection velocity and the adjustment related to higher-order baroclinic Rossby waves. On the other hand, the Atlantic box is located in the west and can be affected by the western boundary coastal Kelvin waves (fast waves). As a contrast, the Pacific box is located in the east so that it is less affected by the fast waves. Therefore, the tropical Atlantic response is faster (because of Kelvin waves), but reaches equilibrium later than the tropical Pacific.

The temperature evolution is closely related to the ocean circulation evolution. However, the evolution time scale of the ocean circulation is much faster than that of the temperature (Fig. 6). In the Pacific, the wind-driven STC adjusts swiftly in response to the external forcing and reaches a new equilibrium in just a few years

(Fig. 6b). This roughly reflects the time scale of interaction between the atmosphere and the slab ocean in the tropics. In the Atlantic, the AMOC changes rapidly in about 20 yr and then evolves slowly to a quasi-equilibrium state in about 80 yr (Fig. 6c). This reflects a quick basin-scale adjustment related to ocean wave dynamics and a slow evolution related to advection and diffusion processes. The main changes in the subsurface ocean temperature occur after the quick adjustment. For example, for the regions interested, during the first 20 yr, the Atlantic subsurface is warmed by only 0.5°C, while after that during years 20–80, it is warmed by more than 3°C (Fig. 6a). This is consistent with the AMOC change and is the consequence of the slow advection and diffusion processes.

It is worth noting that there is an asymmetric change in the AMOC in response to warming and cooling forcings (Fig. 6c). This asymmetry becomes even clearer with the time. In general the AMOC change to cooling forcing (gray line) is much weaker than that to warming forcing (solid black line). During the first 20 yr, the maximum AMOC change is 8 Sv (1 Sv $\equiv 10^6$ m^3 s^{-1}) in the cooling experiment, more than 30% smaller than the 12 Sv in the warming experiment. Moreover, the AMOC is seen undergoing significant recovery in the cooling experiment. It almost returns to the normal 100 yr later. In contrast, the AMOC change in warming experiment stays nearly unchanged after the fulfillment of the ocean adjustment. This asymmetric Atlantic response, that is, the AMOC is more sensitive to the surface warming than the cooling, is determined by the thermodynamic properties of seawater. In the low temperature range, the seawater density change is dominated by the changes in salinity instead of temperature. Therefore, the surface cooling is less efficient than the surface warming to change the AMOC strength. The asymmetric AMOC change can explain the asymmetric temperature change in the tropical subsurface Atlantic very well (Fig. 2b). For example, the corresponding response in −8°C forcing is about −4°C, 50% smaller than the 6°C change in +8°C forcing, consistent with the smaller AMOC change in the cooling experiment (Fig. 6c). In the Pacific, the STC changes in the warming and cooling experiments are symmetric (Fig. 6b), which results in the symmetric temperature in the tropics (Fig. 2b).

4. Mechanisms

a. Different processes in the Atlantic and Pacific

Under the extratropical forcing, the upper-ocean response in the tropical Atlantic is much stronger than that in the tropical Pacific. The former is related to the

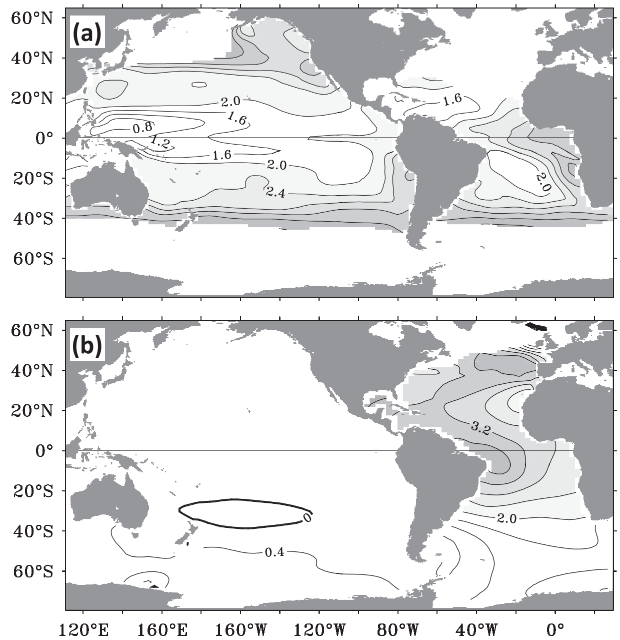

FIG. 7. Temperature changes on (a) $25\sigma_\theta$ and (b) $27.35\sigma_\theta$ levels for the P4 experiment (CI = 0.4°C). The temperature is averaged over years 151–200 and the mean from CTRL is subtracted.

changes in both the Atlantic STC and MOC, while the latter is related to the change in the equatorial cell as well as the shallow subduction process from the Southern Hemisphere. Figure 7 shows the temperature changes on isopycnal levels. On the shallow level (σ_θ = 25, roughly at the depth of 50–200 m), the thermocline warming in the eastern equatorial Pacific can be traced back to the subtropical Southern Hemisphere, suggesting a subduction pathway along the eastern boundary of the Pacific (Fig. 7a). There is a similar eastern thermocline warming in the tropical Atlantic, but this one is weaker than the warming in the west on the deeper layer (Fig. 7b). The temperature change on the 27.35-σ_θ level indicates that the western Atlantic warming is connected to the northern mid- to high latitude through processes along the western boundary, such like the coastal Kelvin waves and the change in the North Brazil Current (NBC). The NBC is a crucial component of the meridional overturning circulation in the low-latitude Atlantic (Fratantoni et al. 2000). The reversal of the NBC from northward to southward can only be accompanied by reducing the strength of the AMOC. The weakening of the AMOC would usually result in a strengthening of the northern branch of the shallow STC in the tropical Atlantic (Fratantoni et al. 2000; Zhang et al. 2003; Hazeleger and Drijfhout 2006; Chang et al. 2008), where the southward NBC consists of the lower branch of the northern STC.

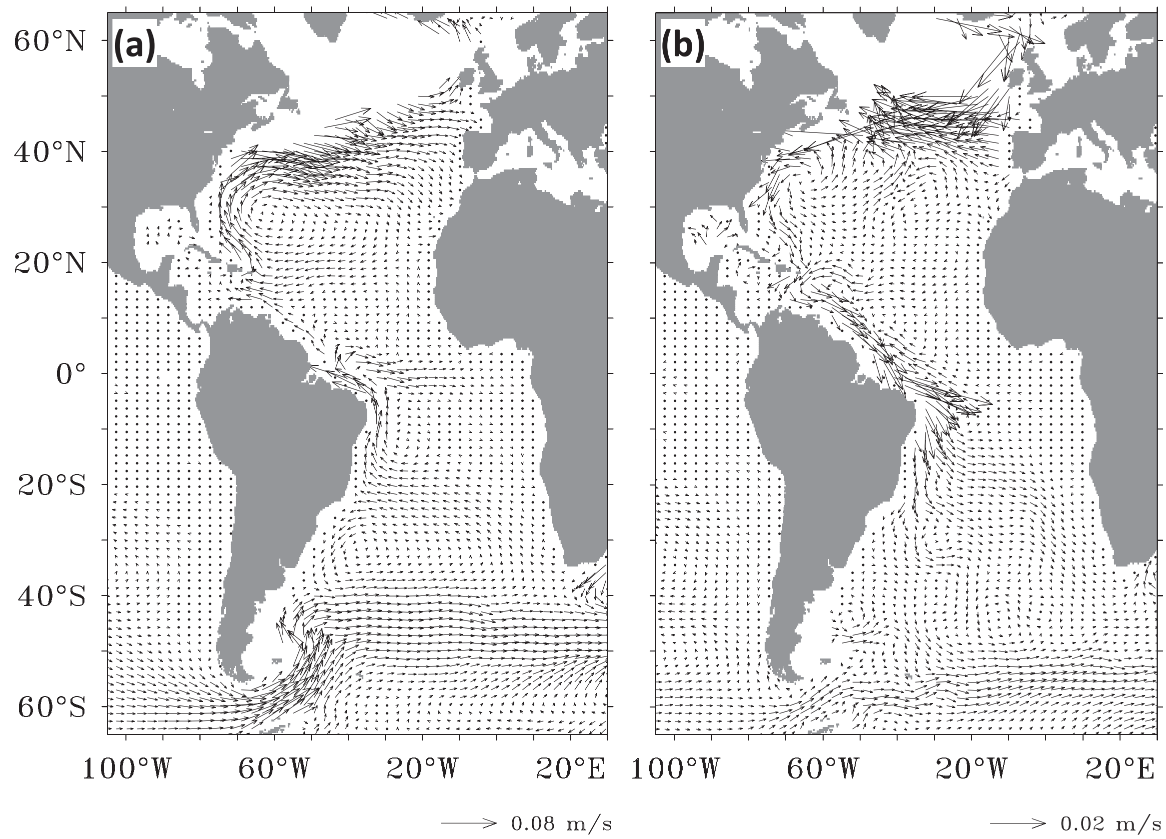

FIG. 8. The Atlantic mean horizontal velocity (a) in the CTRL and (b) its change in the P4 experiment averaged over years 151–200 and between $26.5\sigma_\theta$ and $27.5\sigma_\theta$ levels.

b. Western boundary current change and coastal Kelvin waves in the Atlantic

Consistent with the temperature change shown in Fig. 7b, there is a systematic equatorward anomalous western boundary current in the North Atlantic (Fig. 8b). The western boundary region usually plays as an effective oceanic tunnel connecting the mid- to high latitudes with the equator. This oceanic tunnel is particularly clear in the Atlantic (Fig. 8), while it is less obvious in the Pacific (figure not shown). It is well known that in the North Atlantic there are strong northward western boundary currents, including the NBC in the low latitudes, the Caribbean Current, and the Gulf Stream system as shown in Fig. 8a. Under the extratropical warming forcing, those western boundary currents are weakened significantly as a result of the overall slowdown of the AMOC. The equatorward anomalous Florida Current and the NBC are clearly seen in Fig. 8b.

The changes in the western boundary currents in the North Atlantic are accomplished in terms of coastal Kelvin waves. The Kelvin waves develop quickly and propagate rapidly toward the equator along the western boundary, playing an important role in the equatorward conveying of climate anomalies in the mid- to high latitudes. This process can be viewed vividly in the anomalous field of the temperature and currents. Figure 9 shows the evolution of the temperature and currents on the $27.2\sigma_\theta$ level. The initial response to the extratropical surface warming is a generally weak cooling in the Atlantic thermocline due to the baroclinic adjustment in the upper ocean, which is somehow consistent with what would happen in the Atlantic under the situation of high-latitude water-hosing forcing (e.g., Mignot et al. 2007). Accompanied by the equatorward propagation of the Kelvin waves, the southward anomalous boundary currents first appears between 20° and 40°N (Figs. 9a,b). Then the southward anomalous NBC appears between 0° and 10°N in about 5 yr (Figs. 9c,d). And finally the southward western boundary currents are fully developed in about 20 yr (Figs. 9e–h). Through this process, the extratropical surface warming can reach the equator and cause the significant thermocline warming in the western tropical Atlantic. However, it is noticed that during the first 30 yr and before the fully establishment of the southward anomalous western boundary

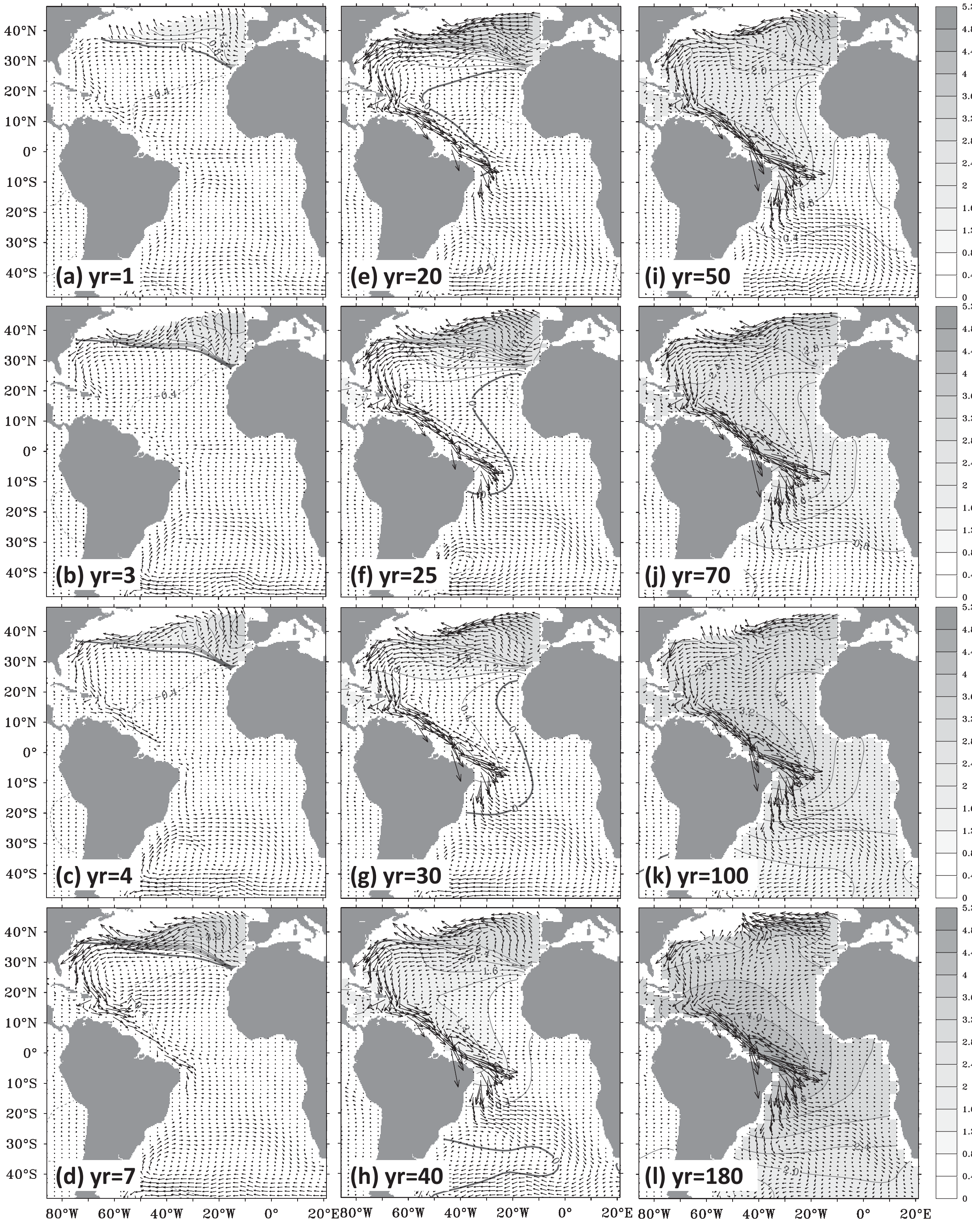

FIG. 9. Snapshots of the temperature (CI = 0.4°C) and velocity (vector) changes on $27.2\sigma_\theta$ level for the P4 experiment. The labels represent the year of the snapshot.

current, the thermocline in the equatorial Atlantic is not warmed too much. It is warmed by less than 0.4°C at year 20 (Fig. 9e). This suggests that although the Kelvin waves are crucial for the initial quick response of the equatorial thermocline to the extratropical forcing, the major change in the equatorial thermocline in the Atlantic occurs after the fully adjustment of the ocean circulation, specifically, after the western boundary current system in the Northern Hemisphere Atlantic is stabilized. This process completes in about 20–30 yr, roughly equal to the time scale of the AMOC adjustment (Fig. 6c). By year 30, the western boundary current as well as the interior current are close to the equilibrium (Fig. 9g), and change little thereafter (Figs. 9g–l). However, the temperature in the tropical Atlantic subsurface keeps rising for a much longer time. For example, in the P4 experiment the temperature along the Brazil coast is increased by 1.2°C at year 40, and further increased to 2.4°C at year 70, 3.2°C at year 100, and 4.0°C at year 180 (Figs. 9j–l). This indicates the continuous warming effect by the advection and diffusion of the warm water from the mid- to high latitudes.

The Kelvin waves' contribution to the initial change in the equatorial Atlantic has been studied in many previous works. Kawase (1987) was the first to study this process in a shallow-water system. Since then there are lots of studies, including GCM simulations forced by freshwater in the mid- to high-latitude Atlantic (e.g., Chang et al. 2008). Freshwater can reduce the deep-ocean convection over the high-latitude North Atlantic, resulting in cold water trapped at the surface layer, causing warming of the subsurface water and stretching of the water column. The local pressure change associated with the warming quickly develops into Kelvin waves that propagate rapidly toward the equator along the western boundary and then along the equatorial waveguide. Here in our coupled model we explicitly see the coastal Kelvin waves, which are also resulted from the oceanic baroclinic adjustment and consistent with the situations in shallow-water system and other GCM simulations. There are also studies on the Kelvin waves' contribution to the equator in the Pacific (e.g., Lysne et al. 1997). However, this process might be trivial because the gaps along the western boundary in the Northern Hemisphere Pacific could result in the leaking of waves' signals into some marginal seas, like the South China Sea, or even into the India Ocean by the Indonesia Throughflow (Rodgers et al. 1999).

The oceanic baroclinic adjustment that is responsible for generating the coastal Kelvin waves can be stirred up by the change in surface wind. Figure 10 shows the mean surface wind curl, the oceanic Ekman pumping, and the net surface heat flux in the CTRL, as well as their changes in the P4 run. In the mean climate, generally there are upwelling in the 40°–60°N of the North Atlantic and downwelling in the 20°–40°S of the South Pacific (Figs. 10a,c). In the warming experiment, these two latitude bands are forced by the anomalous negative wind curl (Fig. 10b), causing anomalous downwelling in the Atlantic and upwelling in the Pacific (Fig. 10d). The anomalous downwelling in the North Atlantic, which is corresponding to the location of the outcropping line of the $27\sigma_\theta$ level, favors the subduction of the surface warming anomaly and pushes the isopycnal level downward at the same time. This process stretches the water column between the $27\sigma_\theta$ and $28\sigma_\theta$ level, generating positive pressure anomaly, which can propagate equatorward along the western boundary in terms of coastal Kelvin waves (Fig. 9), contributing to the maximum temperature change beneath the main thermocline in the equatorial Atlantic. In the Pacific, the anomalous upwelling, or the weakened downwelling between 20° and 40°N/S (Fig. 10d) in the P4 run results in the slowdown of the Pacific STCs in both hemispheres (Fig. 11), which determines the warming in the tropical Pacific. The coastal Kelvin waves in the Pacific should play a trivial role in the tropical mean climate change.

Here we would like to emphasize again that the both the tropical surface and subsurface temperature changes are resulted from the dynamical adjustment of the ocean circulation, instead of the local thermal forcing in the tropics. It is clearly seen that in the P4 run, the net surface heat flux anomaly is negative in the tropics (Fig. 10f), indicating a heat loss from the ocean to the atmosphere, although in the mean climate the tropical oceans gain heat (Fig. 10e). The surface heat flux always plays a damping role in the tropical temperature change (Yang and Liu 2005).

c. *STC versus AMOC*

The significant differences in the tropical response between the Pacific and Atlantic are closely related to the different changes in the meridional overturning circulations as discussed in Fig. 6. Here the detailed structure changes of the circulations are examined. Figure 11 shows the Pacific STC and AMOC changes. In the P4 run, the Pacific STC is weakened by 20% in both the southern and northern branches (Fig. 11b). This is particularly clear in the equatorial cells. In the Atlantic, the deep MOC is also weakened significantly (Fig. 11d). It is well recognized that in a warming world the AMOC will be slowed down in response to the weakening deep-water formation in the high latitudes. This has been simulated by most state-of-the-art climate models in projecting the future climate changes. Besides the weakened AMOC, there is a significant positive change in the tropical upper-ocean circulation between the surface and 600 m in the

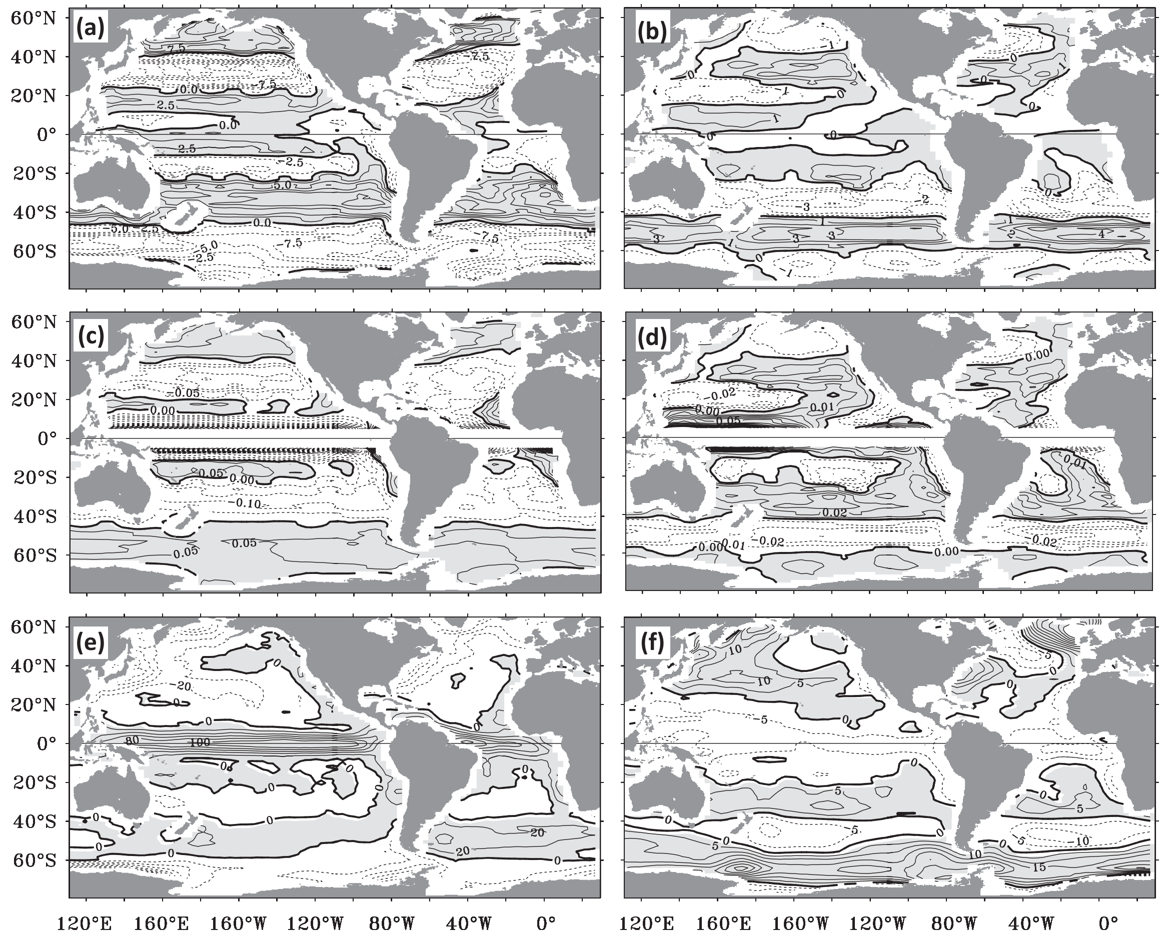

FIG. 10. The mean (a) wind stress curl (CI = 2.5×10^{-8} N m^{-3}), (c) Ekman pumping velocity (CI = 0.05 m day^{-1}) and (e) net oceanic surface heat flux (CI = 20 W m^{-2}) in the CTRL and (b),(d),(f) their changes in the P4 experiment averaged over years 151–200 (CI = 1×10^{-8} N m^{-3}, 0.01 m day^{-1}, and 5 W m^{-2}, respectively). In (c) and (d) the positive (negative) value represents upwelling (downwelling).

P4 run (Fig. 11d). We think this upper-ocean circulation change is the manifestation of the change in the Atlantic STC, which contributes to the upper-ocean temperature change in the tropical Atlantic. It is noticed that the Atlantic STC becomes stronger (weaker) in the Northern (Southern) Hemisphere, remarkably different from the change in the Pacific STC that are weaker in both hemispheres.

The change in the Atlantic STC is a consequence of the weakened AMOC. To better view the Atlantic STC, an enlarged figure of Figs. 11c,d is plotted in Figs. 12a,b. The mean Atlantic STC shows that the southern branch is clear while the northern one is not (Fig. 12a). The arrows in Fig. 12a show the current direction. Previous studies on the interaction between the STC and AMOC have suggested an opposite relationship between them. Indirectly, the AMOC can affect STC through the bridge of the atmosphere. Directly, the AMOC can actually suppress the northern branch of STC (Zhang et al. 2003; Hazeleger and Drijfhout 2006). The STC can also affect the AMOC through advecting anomalous heat and freshwater into the region of the deep-water formation, which can either enhance or shut off the AMOC (Yin and Sarachik 1995). Here we are only interested in the first aspect. Figure 12b exhibits an antisymmetric change in the Atlantic STC: in the P4 experiment the southern branch of the Atlantic STC is weakened, while the northern branch is actually enhanced.

The antisymmetric changes in the Atlantic STC as well as the counterdirection changes in the STC and AMOC in our experiments (Figs. 11–12) are consistent with previous studies. A weakened AMOC would result in an enhanced northern STC, causing the strong and deep response in the tropical Atlantic. An observational study by Zhang et al. (2003) concluded that generally the AMOC tends to reduce the supply of thermocline water to the equator from the North Atlantic and increase the supply from the South Atlantic. They present

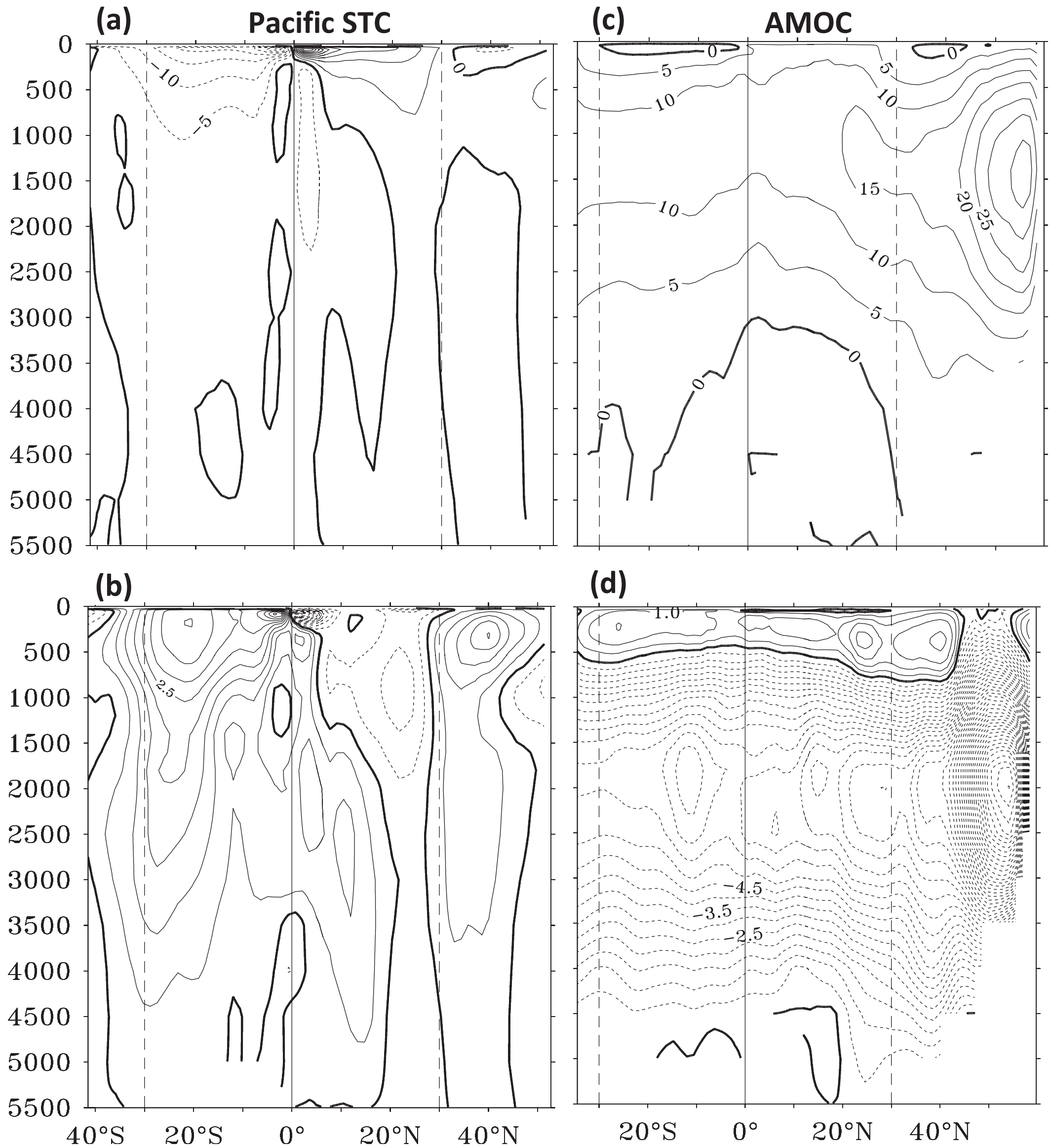

FIG. 11. The mean meridional overturning circulation (CI = 5 Sv) in (a) the Pacific and (c) the Atlantic in the CTRL and (b),(d) their changes in the P4 experiment (CI = 0.5 Sv) averaged over years 151–200.

a schematic figure showing the interaction between the STC and AMOC (figure not shown here). The subsurface equatorward transport by the northern STC is only half of that by the southern STC, mainly due to the counterdirections of the AMOC and the northern STC. A high-resolution ocean modeling study by Hazeleger and Drijfhout (2006) suggests that the weak northern STC is of course a consequence of the AMOC, which prevents much of the subsurface branch of the North Atlantic STC from reaching the equator.

The STC changes in the Atlantic and Pacific are consistent with the temperature changes there. The maximum temperature change in the tropical Atlantic is exclusively related to the change in the northern STC, where the meridional advection plays the dominant role. In Fig. 12b the arrow depicts the anomalous current. The time evolution of this current is also plotted in Fig. 6c (dashed line). During the first stage (years 1–30), the southward anomalous transport is rapidly enhanced because of the weakening AMOC. Thereafter, this transport is weakened slightly because of the effect of the weak northward transport in the interior. In general, the change in the western boundary current dominates the direction and magnitude of the meridional volume transport. As noticed before during the initial stage the temperature change in the tropical Atlantic is only 0.8°C

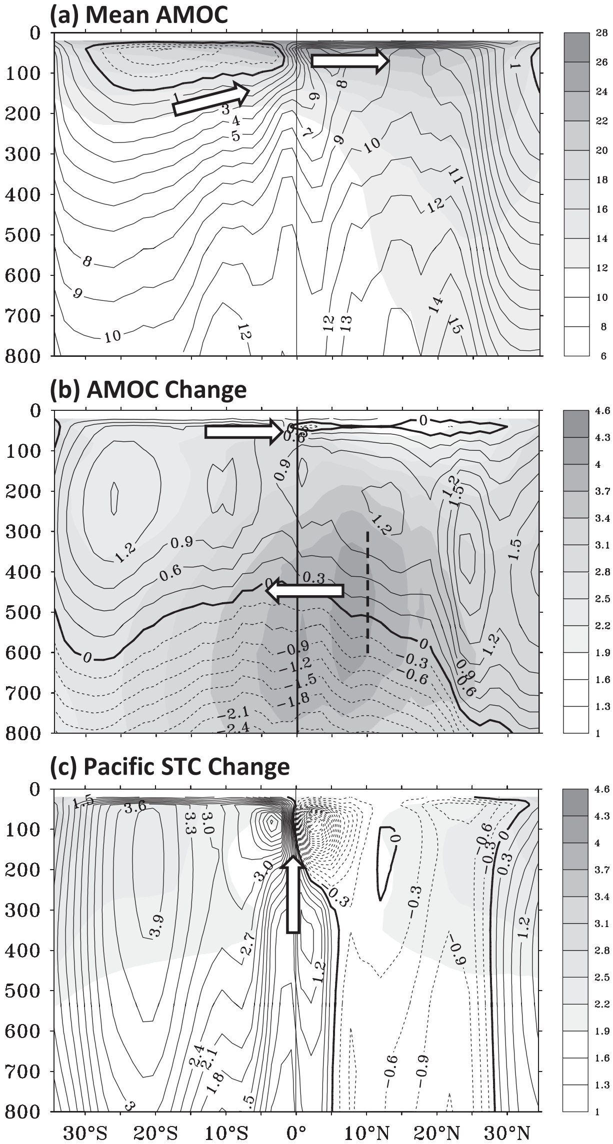

FIG. 12. (a) The mean MOC (contours, CI = 1 Sv) and temperature (filled, CI = 2°C) in the upper Atlantic in the CTRL and (b) the AMOC change (CI = 0.3 Sv) and temperature change (CI = 0.3°C) in the P4 experiment. (c) As in (b), but for the Pacific. Both the circulation and temperature are averaged over years 151–200. The hollow arrows show the direction of transport. The dashed black stick in (b) shows the region where the volume transport is calculated in Fig. 6.

(Fig. 9g). During the quasi-equilibrium stage (after year 30), the temperature change caused by the southward advection, (i.e., the lower branch of the northern STC) is about 4°C (Fig. 12b). The enhanced vertical temperature gradient in Fig. 12b suggests that the vertical advection in the equatorial Atlantic is very weak. In contrast, the relatively uniform upper-ocean temperature change in the equatorial Pacific is primarily a result of change in the vertical advection (Fig. 12c). These are explicitly confirmed by a detailed analysis on the heat budget of the tropical subsurface ocean.

The biggest change in the heat budget of the subsurface box in the equatorial Atlantic (Pacific) comes from the meridional (vertical) advection as depicted in Fig. 13. The subsurface boxes in the Atlantic and Pacific (defined in Fig. 6) represent the regions where the biggest temperature change occurs. In the mean climate, the meridional and vertical advections are the most important stabilized factors for the Atlantic ($-vT_y < 0$) and Pacific ($-wT_z < 0$) (Figs. 13a,b), respectively, which correspond to the strong northward heat transport by the NBC along the western boundary of the tropical Atlantic, and the cold-water upwelling in the eastern equatorial Pacific. In the P4 run, the advections are weakened and become the biggest warming factors [$-(vT_y)' > 0$; $-(wT_z)' > 0$] (blank bars in Figs. 13c,d). The breakdown of the advection terms explicitly shows that the advection changes are predominantly contributed by the perturbation advection components, consistent with the slowdown in the AMOC and Pacific STC. As shown by the black bars in Figs. 13c,d, the perturbation meridional (vertical) advection for the Atlantic (Pacific) box is positive, that is, $-v'T_y > 0$ ($-w'T_z > 0$), where $v' < 0$ and $T_y > 0$ ($w' < 0$ and $T_z > 0$). In the Atlantic the negative v' corresponds to the southward NBC anomaly initiated by the coastal Kelvin waves in the lower thermocline of the western Atlantic (Figs. 8–9). In the Pacific the negative w' corresponds to the weakened upwelling in the eastern equatorial thermocline, which is coherent with the flattening of the equatorial thermocline caused by the weakened Walker circulation. One can refer to Yang and Liu (2005) for the detailed approach calculating heat budget terms.

5. Discussion and conclusions

This work compares the climate changes in the tropical Pacific and Atlantic in response to an idealized extratropical thermal forcing. Although the response magnitudes for the SST are comparable, the overall response patterns are distinct in the two oceans. The temperature change in the tropical Atlantic upper ocean is nearly twice of that in the tropical Pacific. The former has the maximum temperature change located in the west and well below the main thermocline in the equatorial Atlantic. The latter has the maximum change located in the east around the thermocline. The different response patterns result from different processes in the two oceans. In the Pacific, the STC change and the eastern boundary shallow subduction from the extratropical southern Pacific are accountable. In the Atlantic,

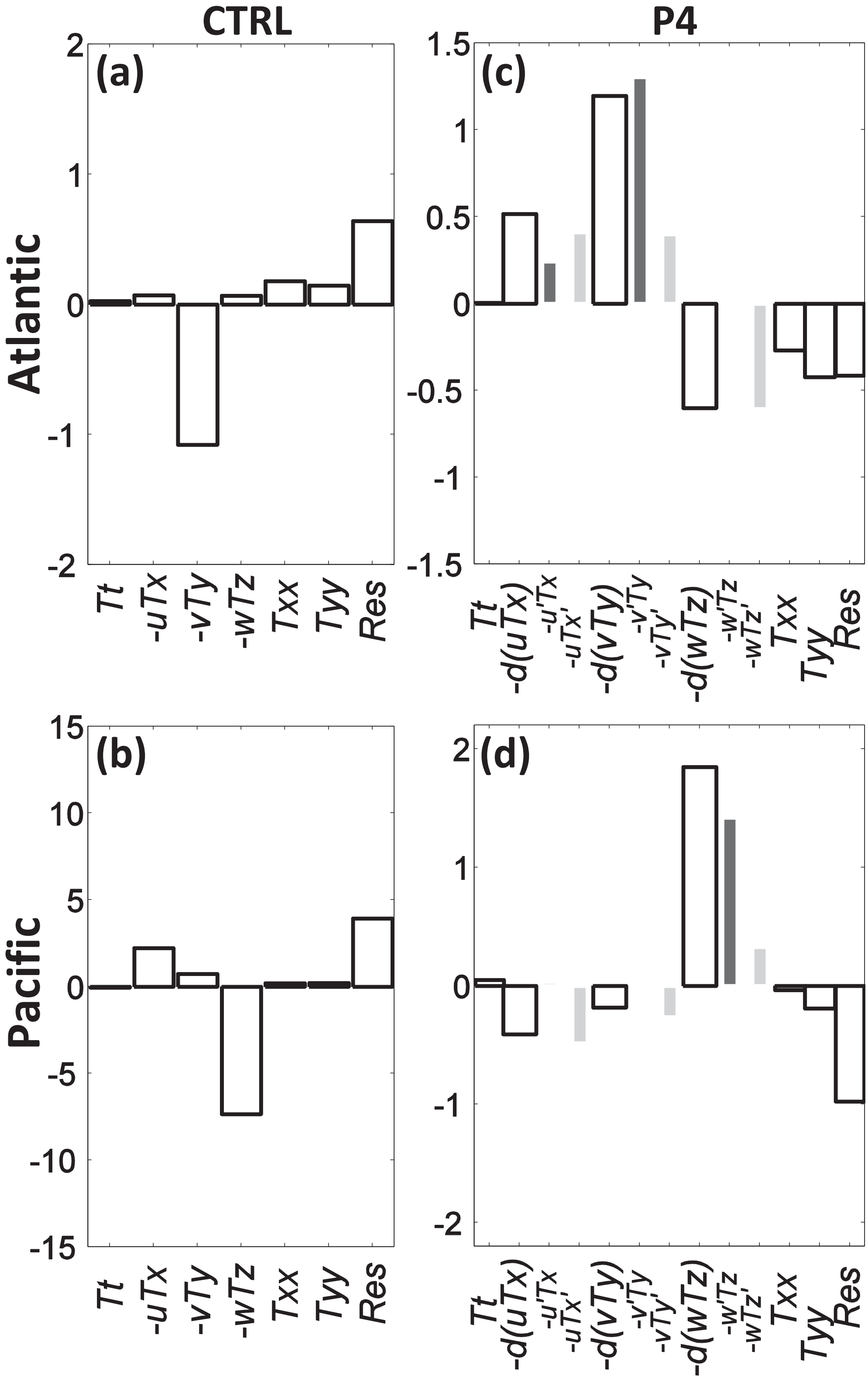

FIG. 13. The temperature budget for the subsurface box of (a) the tropical Atlantic and (b) the tropical Pacific in the CTRL and (c),(d) their changes in the P4 experiment averaged over years 151–200 (blank bars, unit: °C decade^{-1}). The subsurface box is defined in Fig. 6. The total advection changes (blank bars) are decomposed into two components: perturbation advection (black bars) and mean advection (gray bars).

the responsible processes are the changes in the AMOC and the northern STC, as well as the coastal Kelvin waves along the western boundary generated by the anomalous Ekman downwelling in the mid- to high latitudes.

The relative roles of the tropical Atlantic and Pacific in global climate are comparable despite the distinct response patterns. The averaged tropical temperature response is much bigger in the Atlantic than in the Pacific (Fig. 14a); however, the vertical integral of the upper-ocean temperature changes, or, in other words, heat content changes in the two tropical oceans are almost identical (Fig. 14b). The Pacific has the width more than twofold of the Atlantic; thus, the tropical Pacific and Atlantic have comparable weighting in the global climate.

This work focuses more on the climate change in the Atlantic. Usually climate change in the Atlantic is studied by applying freshwater forcing in the high latitudes (Stocker and Wright 1991; Manabe and Stouffer 1995; Mignot et al. 2007; Chang et al. 2008), or changing the atmospheric CO_2 concentration (e.g., Stouffer and Manabe 2003), instead of by prescribing a uniform warming or cooling in the northern North Atlantic. Whatsoever, the tropical Atlantic response to high-latitude thermal forcing in this work is somehow qualitatively consistent with that to high-latitude freshwater forcing. Chang et al. (2008) identified that both the coastal Kelvin wave and the northern STC are responsible for the upper-ocean warming in the equatorial Atlantic in their water-hosing-coupled model simulations. The wave adjustment contributes only to the initial weak warming. The appearance of the northern STC causes the rapid warming after 20–25 yr. These two different ocean dynamics control the two stages of warming in the equatorial Atlantic. In our experiment, the two ocean processes are also identified. The coastal Kelvin waves are particularly clear on the 27–28σ_θ level, which corresponds to the depth of lower thermocline and the intermediate water in the North Atlantic. The change in the northern STC is also significant, with the influence extending downward to 600–800-m depth in the tropics. The major change in the equatorial Atlantic occurs only after the full establishment of the northern STC, specifically the lower equatorward limb of the northern STC.

A major difference between our thermal forcing experiment and the freshwater forcing simulation is that the wind-driven STC in the Atlantic can show up explicitly in the latter experiments (Fig. 2b in Chang et al. 2008). The AMOC suppresses the northern STC to a great extent, which on the contrary implies that shutting down the AMOC would result in a visible closed northern STC. Adding a 0.6-Sv freshwater (equivalent to a salinity decrease by 10–15 psu) in the high-latitude Atlantic can reduce the Northern Hemisphere AMOC by as much as 80%–90% (Chang et al. 2008), so that the Atlantic STCs show a nearly antisymmetric structure similar to the Pacific STCs within the tropics. In our thermal forcing experiments, the Northern Hemisphere AMOC is weakened by 20% for a 4°C warming (Figs. 11c,d) and 50% for an 8°C warming (figure not shown). Although this surface warming in the high-latitude Atlantic plays the similar role as the freshwater in reducing the surface water density, enhancing the vertical stratification and weakening the deep-water formation there, the efficiency of the thermal expansion is much lower than that of the saline contraction in changing the potential density in the North Atlantic. In the low-temperature range (0°–10°C), the saline contraction is about 4–8 times efficient than the thermal expansion in the density change as predicted by the Gibbs thermodynamic potential function of seawater (Feistel 2005). Therefore, the warming alone in the high latitude is hard to shut down the AMOC completely, so that a closed northern STC can be still invisible. Another critical factor to the STC strength is the surface wind forcing in the midlatitudes. In Chang et al. (2008) the midlatitude westerlies are strengthened significantly because of the strong cooling in the North Atlantic SST. In contrast, the

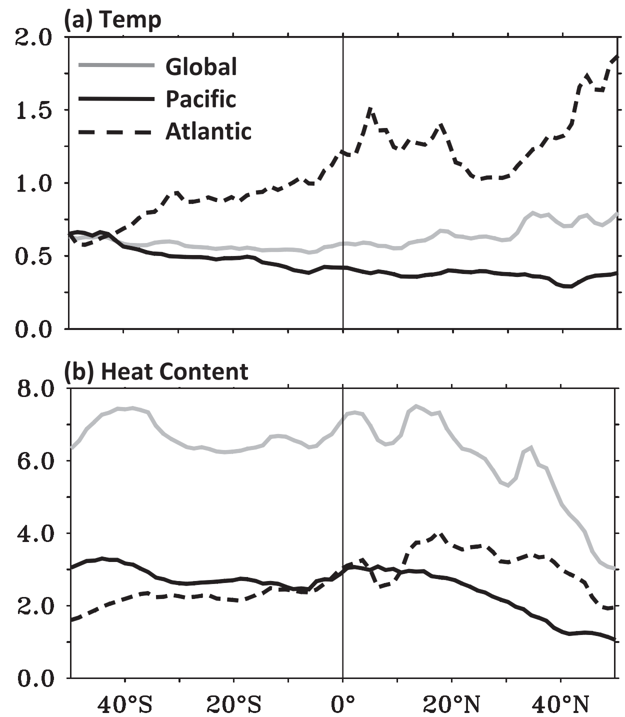

FIG. 14. The linear responses of (a) the averaged temperature anomalies (unit: °C) and (b) the heat content anomalies (unit: 10^{10} °C m^{-2}, averaged over 0–5500 m) based on P4/M4 experiments. Solid black, dashed black, and gray lines represent the Pacific, Atlantic, and global oceans, respectively.

midlatitude westerlies are weakened significantly in our experiments, so are the Hadley cells and the wind-driven ocean circulations (Yang and Liu 2005). Therefore, the northern STC in the Atlantic is not as clear as that in the water-hosing simulations, although the AMOC is weakened significantly indeed.

The climate change in a warming world should be much more complicate than the scenario suggested in either the thermal or freshwater forcing simulation. A warming in the high latitudes should be also accompanied by sea ice melting, that is, freshening in the high latitudes. This implies that a coupled climate model without a reasonable sea ice dynamics or thermodynamics would hardly succeed in simulating the realistic change in a warming or cooling world. It is recognized that the global mean temperature has been risen by 1°–1.5°C over the past century, in which more warming occurs in the high latitudes. Accordingly, the MOC is thought to be slowed down (McPhaden and Zhang 2002; Bryden et al. 2005). However, a recent observational study found that the Atlantic AMOC has became stronger over the past five decades due to the enhanced equator–pole density difference, although the temperature difference is weakened (Wang et al. 2010a). Because of the opposite effects of temperature and salinity on density, there is a big uncertainty in the future change in the AMOC. This could affect the global climate variability on all time scales. Apparently a coupled model with reasonable sea ice module is the preliminary step to approach the reality.

Of course, our coupled model experiments have some problems. First of all, the idealized uniform extratropical forcing is not as real as that could happen in the reality. Second, the magnitude of the imposed forcing is out of the possible climate change range in the near future. Third, the feedback of the tropical climate change to the extratropics is mandatorily suppressed in order to focus on the passive response of the tropical climate. Forth, in this work we also fail to identify the interbasin interaction between the Atlantic and Pacific. This could be substantial as suggested in Wang et al. (2010b), in which a significant fingerprint of the Atlantic warm pool in the southeastern Pacific is identified. In our experiments, the Atlantic warm pool could also impact the tropical Pacific and vice versa. Besides, the change in extratropical Atlantic (Pacific) can affect the tropical Pacific (Atlantic) considerably. Fifth, to separate the STC and AMOC influence on the tropical Atlantic, trajectory analyses on the mass transport should be used. Finally, in this work we did not give detailed analyses on the responses in the tropical Pacific as well as corresponding adjustment in the ocean circulation such like the Pacific STC. One can refer to our previous work for details (Yang and Liu 2005).

It is uncertain if our results would be also valid in other models. There are some different modeling studies using the similar approach (e.g., Matei et al. 2008; Yu and Sun 2009), which suggest similar mechanisms of extratropical forced tropical variability. Notwithstanding, this work provides an valuable quantitative estimate of the tropical ocean response to extratropical forcing, as well as the relative roles of the tropical Atlantic and Pacific in global climate. It also suggests an approach in studying the climate interaction among different regions, different climate systems, or processes as well.

Acknowledgments. This work is jointly supported by the NSF of China (Grants 40576004 and 40976007), the National Basic Research Program of China (Grant 2007CB411801), and the Norwegian Research Council through the East Asian DecCen project (193690/S30). All the experiments are performed on the supercomputer in the Peking University.

REFERENCES

Alexander, M. A., I. Blade, M. Newman, J. R. Lanzante, N.-C. Lau, and J. D. Scott, 2002: The atmospheric bridge: The influence of ENSO teleconnections on air–sea interaction over the global oceans. *J. Climate,* **15,** 2205–2231.

Barnett, T., D. W. Pierce, M. Latif, D. Dommenget, and R. Saravana, 1999: Interdecadal interactions between the tropics and the midlatitudes in the Pacific basin. *Geophys. Res. Lett.,* **26,** 615–618.

Bryden, H. L., H. R. Longworth, and S. A. Cunningham, 2005: Slowing of the Atlantic meridional overturning circulation at 25°N. *Nature,* **438,** 655–657.

Cane, M. A., A. C. Clement, A. Kaplan, Y. Kushnir, D. Pozdnyakov, R. Seager, S. E. Zebiak, and R. Murtugudde, 1997: Twentieth-century sea surface temperature trends. *Science,* **275,** 957–960.

Chang, P., and Coauthors, 2008: Oceanic link between abrupt changes in the North Atlantic Ocean and the African monsoon. *Nat. Geosci.,* **1,** 444–448.

Clement, A. C., R. Seager, M. A. Cane, and S. E. Zebiak, 1996: An ocean dynamic thermostat. *J. Climate,* **9,** 2190–2196.

Curry, R. G., M. S. McCartney, and T. M. Joyce, 1998: Oceanic transport of subpolar climate signals to mid-depth subtropical waters. *Nature,* **391,** 575–577.

Enfield, D. B., and D. A. Mayer, 1997: Tropical Atlantic sea surface temperature variability and its relation to El Niño–Southern Oscillation. *J. Geophys. Res.,* **102,** 929–945.

Feistel, R., 2005: Numerical implementation and oceanographic application of the Gibbs thermodynamic potential of seawater. *Ocean Sci.,* **1,** 9–16.

Fratantoni, D. M., W. E. Johns, T. L. Townsend, and H. E. Hurlburt, 2000: Low-latitude circulation and mass transport pathways in a model of tropical Atlantic Ocean. *J. Phys. Oceanogr.,* **30,** 1944–1966.

Gu, D., and S. G. H. Philander, 1997: Interdecadal climate fluctuations that depend on exchanges between the tropics and extratropics. *Science,* **275,** 805–807.

Hazeleger, W., and S. Drijfhout, 2006: Subtropical cells and meridional overturning circulation pathways in the tropical Atlantic. *J. Geophys. Res.,* **111,** C03013, doi:10.1029/2005JC002942.

Hoerling, M. P., J. W. Hurrell, and T. Xu, 2001: Tropical origins for recent North Atlantic climate change. *Science,* **292,** 90–92.

Jacob, R. L., 1997: Low frequency variability in a simulated atmosphere–ocean system. Ph.D. thesis, University of Wisconsin—Madison, 155 pp.

Kawase, M., 1987: Establishment of deep ocean circulation driven by deep-water production. *J. Phys. Oceanogr.,* **17,** 2297–2317.

Kleeman, R., J. P. McCreary, and B. A. Klinger, 1999: A mechanism for generating ENSO decadal variability. *Geophys. Res. Lett.,* **26,** 1743–1746.

Lau, N.-C., 1997: Interactions between global SST anomalies and the midlatitude atmospheric circulation. *Bull. Amer. Meteor. Soc.,* **78,** 21–33.

Liu, Z., and H. Yang, 2003: Extratropical control of tropical climate, the atmospheric bridge and oceanic tunnel. *Geophys. Res. Lett.,* **30,** 1230, doi:10.1029/2002GL016492.

——, S. Vavrus, F. He, N. Wen, and Y. Zhong, 2005: Rethinking tropical ocean response to global warming: The enhanced equatorial warming. *J. Climate,* **18,** 4684–4700.

Lu, J., R. J. Greatbatch, and K. A. Peterson, 2004: Trend in Northern Hemisphere winter atmospheric circulation during the last half of the twentieth century. *J. Climate,* **17,** 3745–3760.

Lysne, J., P. Chang, and B. Giese, 1997: Impact of the extratropical Pacific on equatorial variability. *Geophys. Res. Lett.,* **24,** 2589–2592.

Manabe, S., and R. J. Stouffer, 1995: Simulation of abrupt climate change induced by freshwater input to the North Atlantic Ocean. *Nature,* **378,** 165–167.

Matei, D., N. Keenlyside, M. Latif, and J. Jungclaus, 2008: Subtropical forcing of tropical Pacific climate and decadal ENSO modulation. *J. Climate,* **21,** 4691–4709.

McCreary, J., and P. Lu, 1994: On the interaction between the subtropical and the equatorial oceans: The subtropical cell. *J. Phys. Oceanogr.,* **24,** 466–497.

McPhaden, M. J., and D. X. Zhang, 2002: Slowdown of the meridional overturning circulation in the upper Pacific Ocean. *Nature,* **415,** 603–608.

Mignot, J., A. Ganopolski, and A. Levermann, 2007: Atlantic subsurface temperatures: Response to a shutdown of the overturning circulation and consequences for its recovery. *J. Climate,* **20,** 4884–4898.

Nonaka, M., S.-P. Xie, and J. P. McCreary, 2002: Decadal variations in the subtropical cells and equatorial Pacific SST. *Geophys. Res. Lett.,* **29,** 1116, doi:10.1029/2001GL013717.

Pierce, D. W., T. P. Barnett, and M. Latif, 2000: Connections between the Pacific Ocean tropics and midlatitudes on decadal timescales. *J. Climate,* **13,** 1173–1194.

Rodgers, K., M. A. Cane, N. Naik, and D. Schrag, 1999: The role of the Indonesian throughflow in equatorial Pacific thermocline ventilation. *J. Geophys. Res.,* **104,** 20 551–20 570.

Schneider, E. K., R. S. Lindzen, and B. P. Kirtman, 1997: A tropical influence on global climate. *J. Atmos. Sci.,* **54,** 1349–1358.

Stocker, T. F., and D. G. Wright, 1991: Rapid transitions of the ocean's deep circulation induced by changes in the surface water fluxes. *Nature,* **351,** 729–732.

Stouffer, R. J., and S. Manabe, 2003: Equilibrium response of thermohaline circulation to large changes in atmospheric CO_2 concentration. *Climate Dyn.,* **20,** 759–773.

Sutton, R. T., and D. L. R. Hodson, 2007: Climate response to basin-scale warming and cooling of the North Atlantic Ocean. *J. Climate,* **20,** 891–907.

Wang, C., 2002: Atmospheric circulation cells associated with the El Niño–Southern Oscillation. *J. Climate,* **15,** 399–419.

——, S. Dong, and E. Munoz, 2010a: Seawater density variations in the North Atlantic and the Atlantic meridional overturning circulation. *Climate Dyn.,* **34,** 953–968, doi:10.1007/s00382-009-0560-5.

——, S.-K. Lee, and C. R. Mechoso, 2010b: Interhemispheric influence of the Atlantic warm pool on the southeastern Pacific. *J. Climate,* **23,** 404–418.

Wu, L., Z. Liu, R. Gallimore, R. Jacob, D. Lee, and Y. Zhong, 2003: Pacific decadal variability: The tropical Pacific mode and the North Pacific mode. *J. Climate,* **16,** 1101–1120.

Yang, H., and Z. Liu, 2005: Tropical-extratropical climate interaction as revealed in idealized coupled climate model experiments. *Climate Dyn.,* **24,** 863–879.

——, and L. Wang, 2008: Estimating the nonlinear response of tropical ocean to extratropical forcing in a coupled climate model. *Geophys. Res. Lett.,* **35,** L15705, doi:10.1029/2008GL034256.

——, and Q. Zhang, 2008: Anatomizing the ocean role in ENSO changes under global warming. *J. Climate,* **21,** 6539–6555.

——, H. Jiang, and B. Tan, 2005: Asymmetric impact of the North and South Pacific on the equator in a coupled climate model. *Geophys. Res. Lett.,* **32,** L05604, doi:10.1029/2004GL021925.

Yin, F. Y., and E. S. Sarachik, 1995: Interdecadal thermohaline oscillations in a sector ocean general circulation model: Advective and convective processes. *J. Phys. Oceanogr.,* **25,** 2465–2484.

Yu, L., and M. M. Rienecker, 1999: Mechanisms for the Indian Ocean warming during 1997-1998 El Niño. *Geophys. Res. Lett.,* **26,** 735–738.

Yu, Y., and D.-Z. Sun, 2009: Response of ENSO and the mean state of the tropical Pacific to extratropical cooling and warming: A study using the IAP coupled model. *J. Climate,* **22,** 5902–5917.

Zhang, D. X., M. J. McPhaden, and W. E. Johns, 2003: Observational evidence for flow between the subtropical and tropical Atlantic: The Atlantic subtropical cells. *J. Phys. Oceanogr.,* **33,** 1783–1797.

——, R. Msadek, M. J. McPhaden, and T. Delworth, 2011: Multidecadal variability of the North Brazil Current and its connection to the Atlantic meridional overturning circulation. *J. Geophys. Res.,* in press, doi:10.1029/2010JC006812.

Zhang, R., and T. Delworth, 2006: Impact of Atlantic multidecadal oscillations on India/Sahel rainfall and Atlantic hurricanes. *Geophys. Res. Lett.,* **33,** L17712, doi:10.1029/2006GL026267.

Zhang, X., J. Sheng, and A. Shabbar, 1998: Modes of interannual and interdecadal variability of Pacific SST. *J. Climate,* **11,** 2556–2569.

Zhang, Y., J. M. Wallace, and N. Iwasaka, 1996: Is climate variability over the North Pacific a linear response to ENSO? *J. Climate,* **9,** 1468–1478.